Electronic Supplementary Material (ESI) for Journal of Materials Chemistry A.

Electronic supplementary information (ESI)

Nitrogen, Phosphorus Co-doped Eave-like Hierarchical Porous Carbon for Efficient Capacitive Deionization

Hao Zhang[1], Chaohai Wang[1], Wuxiang Zhang[1], Ming Zhang[1], Junwen Qi[1], Jieshu Qian[1], Xiuyun Sun[1], Brian Yuliarto[2,3], Jongbeom Na[4], Teahoon Park[5], Hassannien Gomaa Abdien Gomaa[6], Yusuf Valentino Kaneti[4], Jin Woo Yi[5]*, Yusuke Yamauchi[4,7], Jiansheng Li[1]**

[1] Key Laboratory of Jiangsu Province for Chemical Pollution Control and Resources Reuse, School of Environmental and Biological Engineering, Nanjing University of Science and Technology, Nanjing 210094, China

[2] Advanced Functional Materials Laboratory, Department of Engineering Physics, Institute of Technology Bandung, Bandung 40132, Indonesia

[3] Research Center for Nanosciences and Nanotechnology (RCNN), Institute of Technology Bandung, Bandung 40132, Indonesia

[4] Australian Institute for Bioengineering and Nanotechnology (AIBN) and School of Chemical Engineering, The University of Queensland, Brisbane, Queensland 4072, Australia

[5] Carbon Composite Department, Composites Research Division, Korea Institute of Materials Science (KIMS), Changwon-si 51508, Gyeongsangnam-do, Republic of Korea

[6] Chemistry Department, Faculty of Science, Al-Azhar University, Assiut 71524, Egypt

[7] JST-ERATO Yamauchi Materials Space-Tectonics Project and International Research Center for Materials Nanoarchitectonics (WPI-MANA), National Institute for Materials Science (NIMS), Tsukuba, Ibaraki 305-0044, Japan

E-mails: v.kaneti@uq.edu.au; yjw0628@kims.re.kr; lijsh@njust.edu.cn

Table. S1. Structural parameters and elemental compositions of ZIF-8-C, N-EPC, and NP-EHPC.

Sample	S_{BET} (m^2 g^{-1})	V_{pore} (cm^3 g^{-1})	V_{micro} (cm^3 g^{-1})	V_{micro}/V_{pore}	Elemental composition (%)				N/P ratio
					C	O	N	P	
ZIF-8-C	1044.0	0.49	0.45	0.92	78.1	6.8	15.1	--	--
N-EPC	1065.7	0.60	0.28	0.47	84.5	5.9	9.6	--	--
NP-EHPC	1165.8	0.72	0.13	0.18	78.6	16.8	2.9	1.7	1.71
NP-EHPC-65	983.5	0.66	0.16	0.24	80.3	10.9	5.7	3.1	1.84
NP-EHPC-195	1155.5	0.82	0.18	0.22	82.1	12.4	3.0	2.5	1.20

Table. S2. R_s and R_{ct} values of ZIF-8-C, N-EPC, and NP-EHPC electrodes.

Sample	R_s (Ω)	R_{ct} (Ω)
ZIF-8-C	3.49	3.48
N-EPC	3.36	3.19
NP-EHPC	2.92	1.65

Table. S3. Comparison of desalination capacities of reported carbon materials.

Electrode materials	Applied voltage (V)	Initial NaCl concentration (mg L^{-1})	SAC (mg g^{-1})	Cycle number	Ref.
Nitrogen-doped CNFA800	1.2	500	14.3	10 (~100%)	1
Graphite reinforced-cellulose (GrC)	1.2	500	13.1	10 (~99%)	2
ZIF-8@PZS-C	1.2	500	22.19	20 (~98%)	3
Graphene aerogel (GA)	1.2	500	9.9	/	4
ZIF-67/PPy hybrid	1.2	584	11.34	100 (~98%)	5
Nitrogen-doped porous carbon tubes composite ($PCT_{1.75}$-N)	1.2	500	16.7	100 (92.5%)	6
Nitrogen-doped carbon/rGO nano-sandwiches	1.2	589	17.52	10 (~99%)	7
Hierarchically porous 3D architectural graphene (GO-Mw-Hyd)	1.0	500	4.79	3 (~83%)	8
Activated carbon	1.0	500	11.0	/	9
Porous carbon fibers	1.0	500	30.4	30 (~98%)	9
Open and interconnected porous architectures (3DGA-OP)	1.2	500	14.35	15 (~99%)	10
Nitrogen-doped activated carbon	1.2	468	24.7	100 (~40%)	11
Iron-nitrogen-doped carbon nanoparticles	1.2	293	8	200 (~68.7%)	12
Ordered microporous carbon	0.8	2000	15.75	200 (~50%)	13
Sugarcane Biowaste-Derived Biochars	1.2	600	21.8	70 (~87%)	14
NP-EHPC	1.2	500	24.14	150 (~74%)	This work

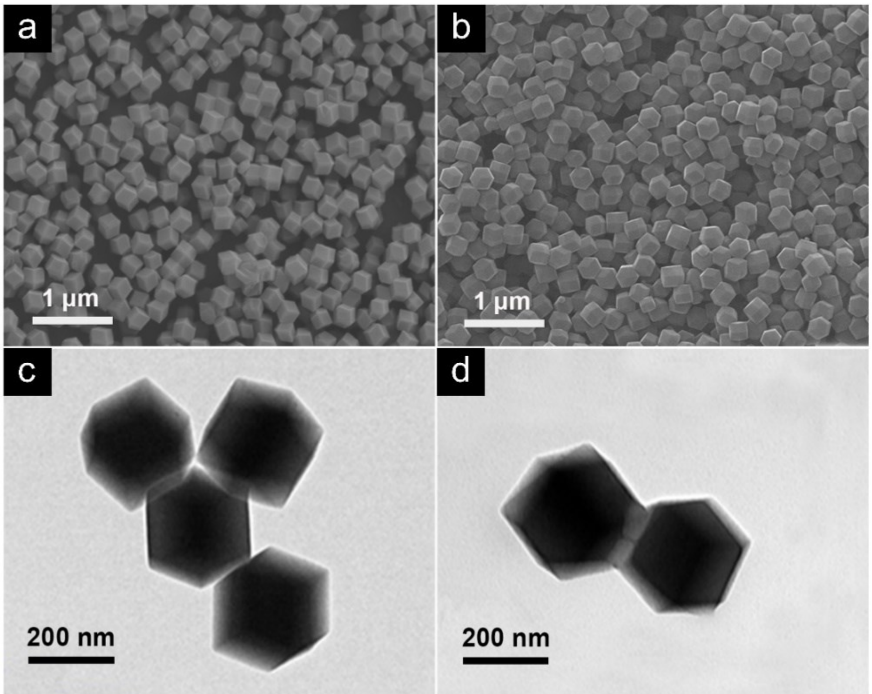

Fig. S1. SEM and TEM images of (a, c) ZIF-8 and (b, d) ZIF-8@AF.

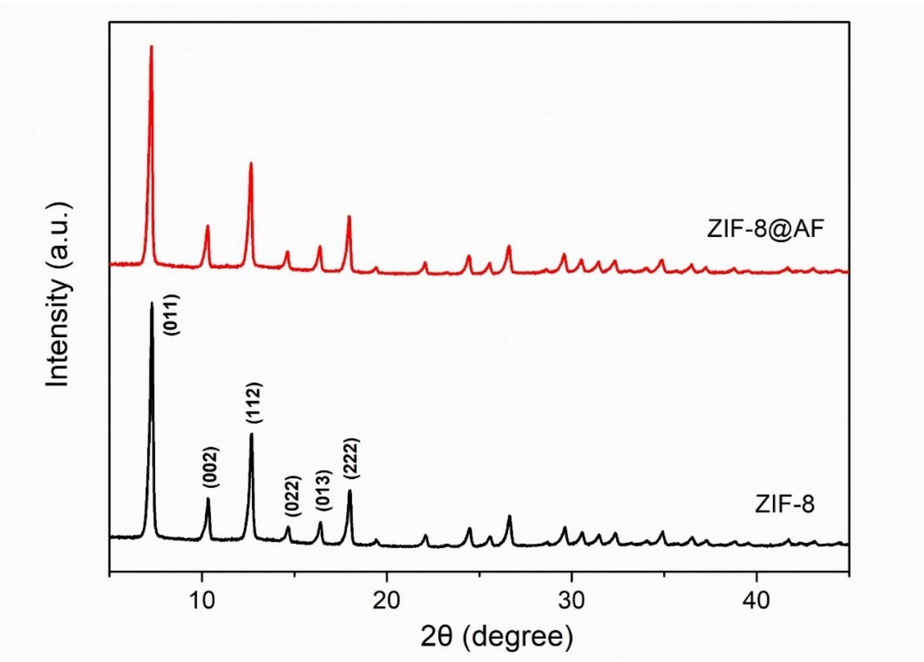

Fig. S2. XRD patterns of ZIF-8 and ZIF-8@AF.

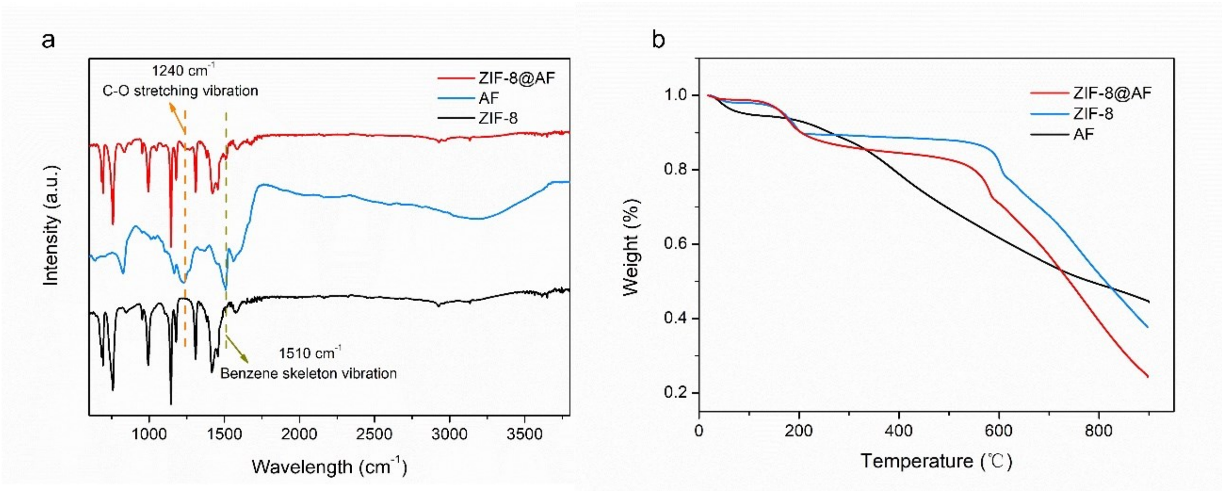

Fig. S3. (a) IR spectra of AF, ZIF-8, and ZIF-8@AF. (b) TG curves of AF, ZIF-8, and ZIF-8@AF in N_2 atmosphere at a heating rate of 5 °C min^{-1}.

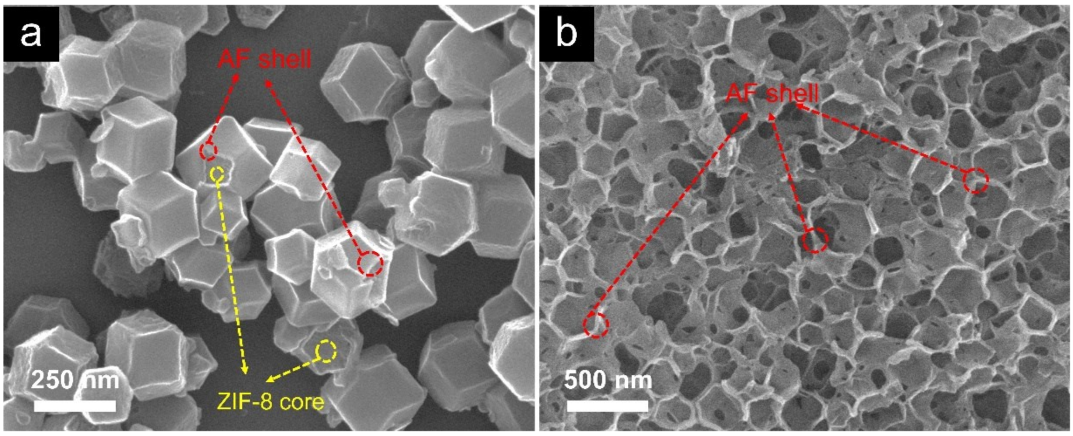

Fig. S4. SEM images of ZIF-8@AF after acid etching with (a) pH = 2 and (b) pH = 1.

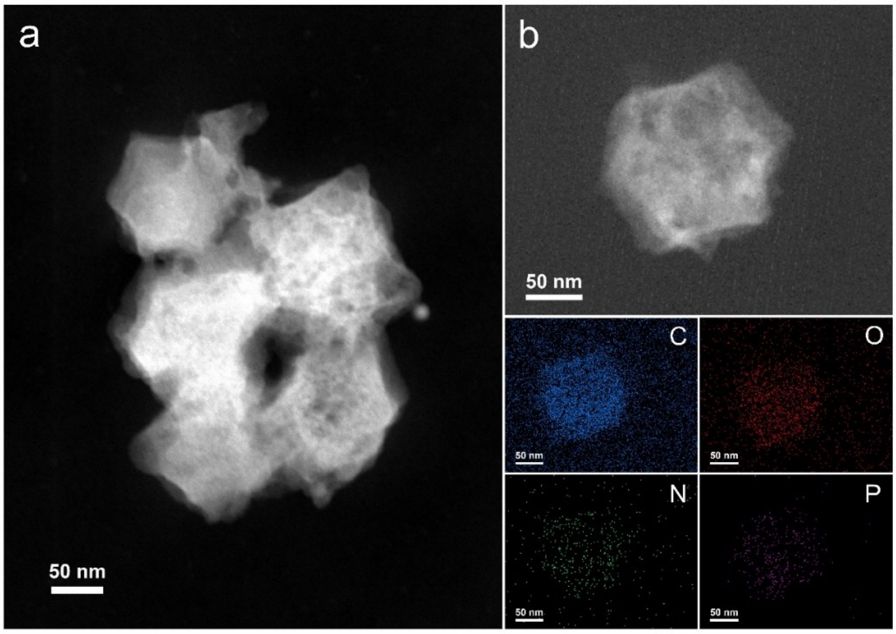

Fig. S5. (a) HAADF-STEM image and (b) the corresponding EDS elemental mapping of NP-EHPC.

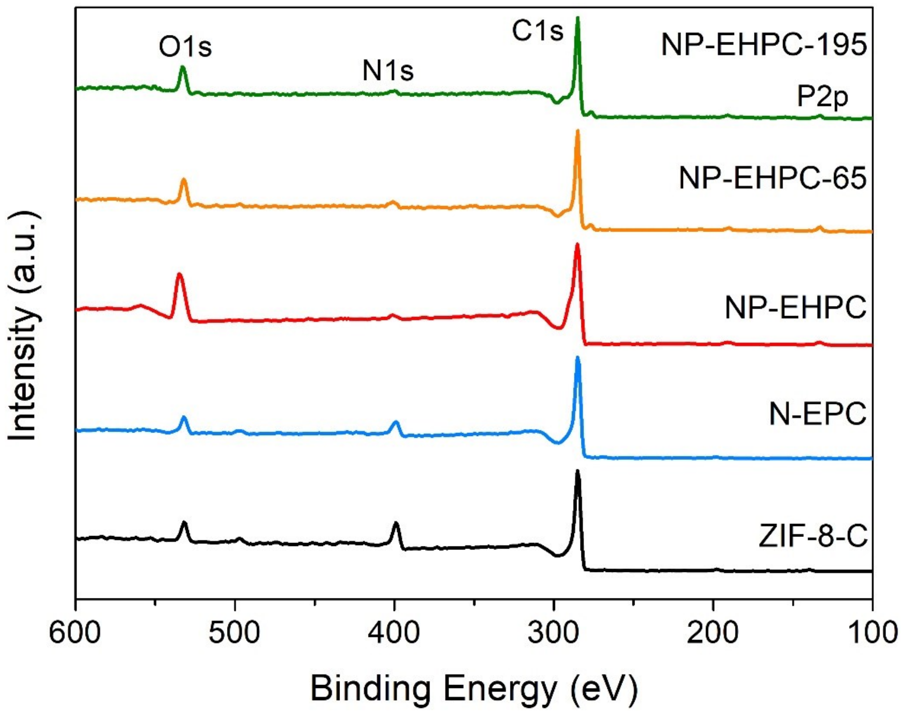

Fig. S6. XPS survey spectra of ZIF-8-C, N-EPC, NP-EHPC, NP-EHPC-65, and NP-EHPC-195.

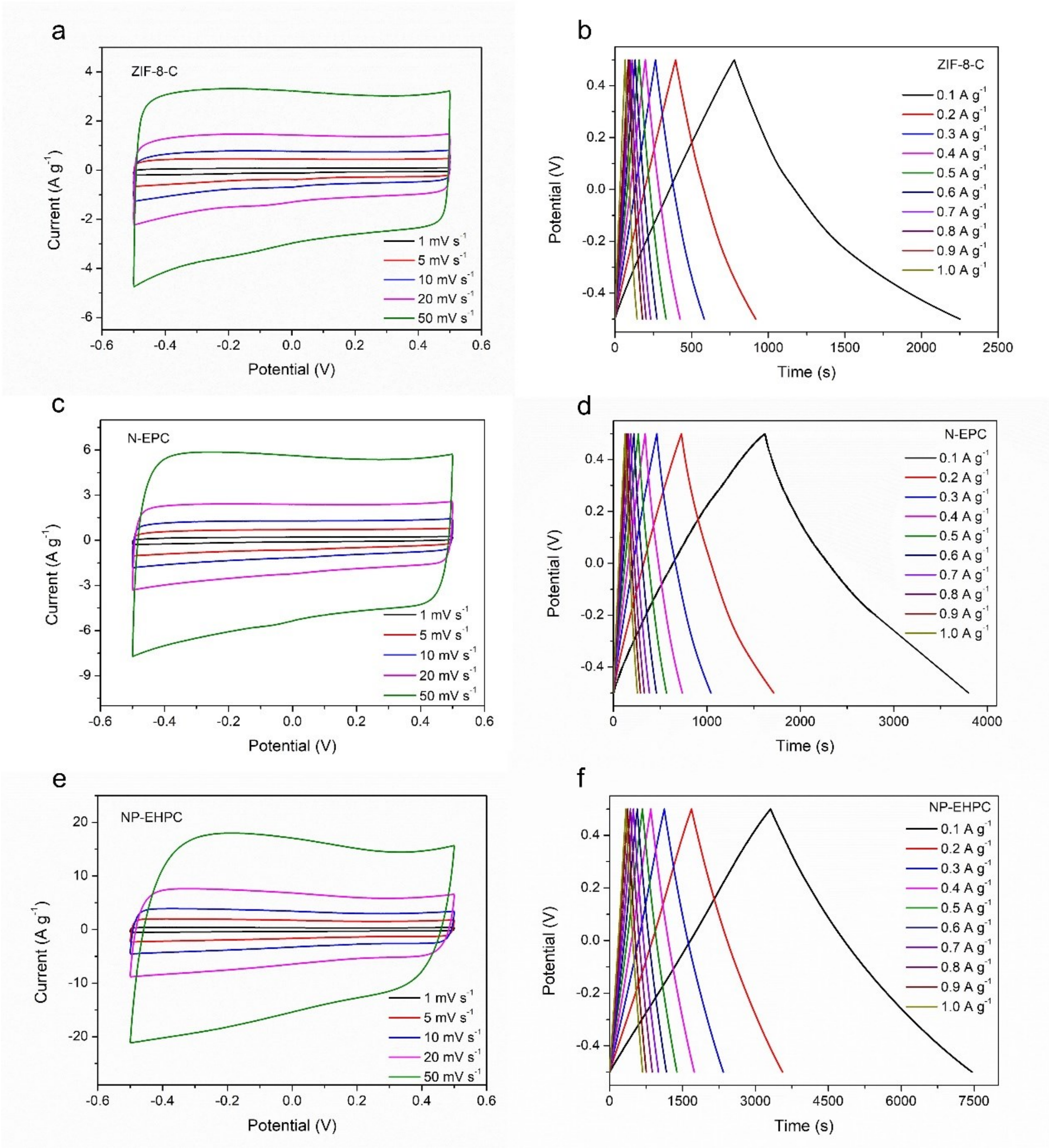

Fig. S7. CV curves and GCD plots of (a, b) ZIF-8-C, (c, d) N-EPC, and (e, f) NP-EHPC at different scan rates and current densities in 1 M NaCl solution.

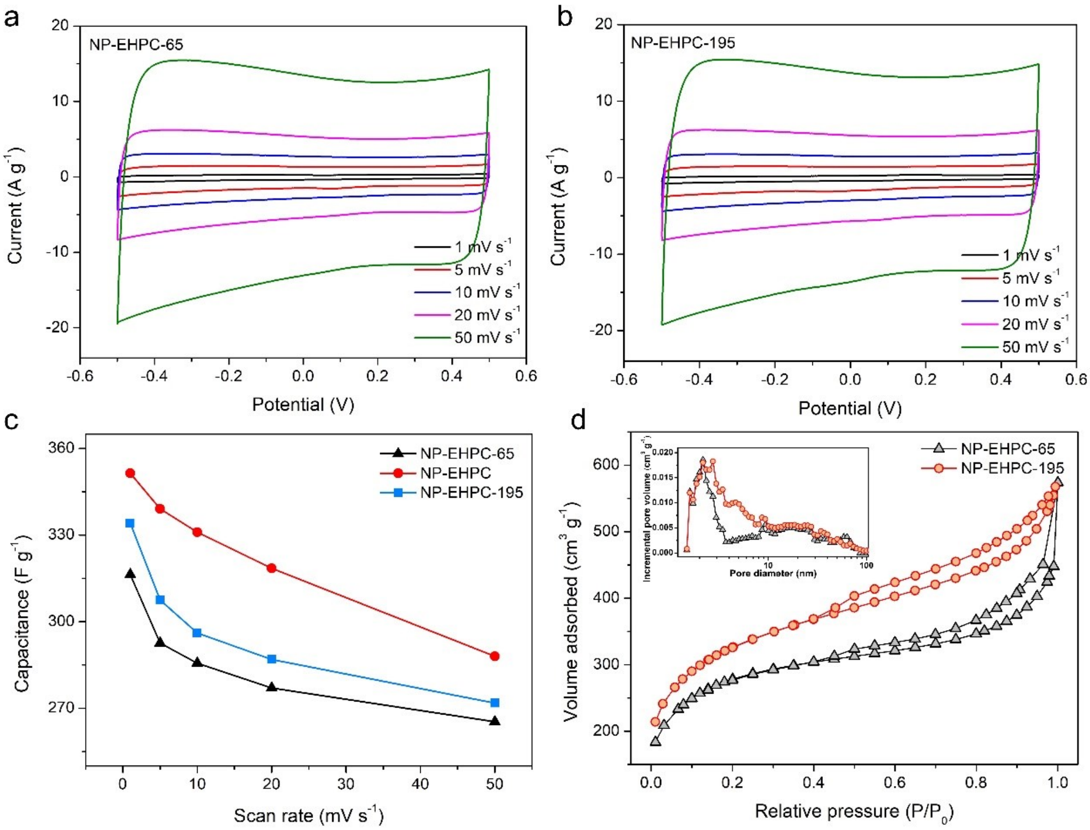

Fig. S8. CV curves of (a) NP-EHPC-65 and (b) NP-EHPC-195 at different scan rates in 1 M NaCl solution. (c) The specific capacitance values of NP-EHPC-65, NP-EHPC, and NP-EHPC-195 at different scan rates from 1 to 50 mV s^{-1}. (d) N_2 adsorption-desorption isotherms and pore diameter distribution curves (inset) of NP-EHPC-65 and NP-EHPC-195.

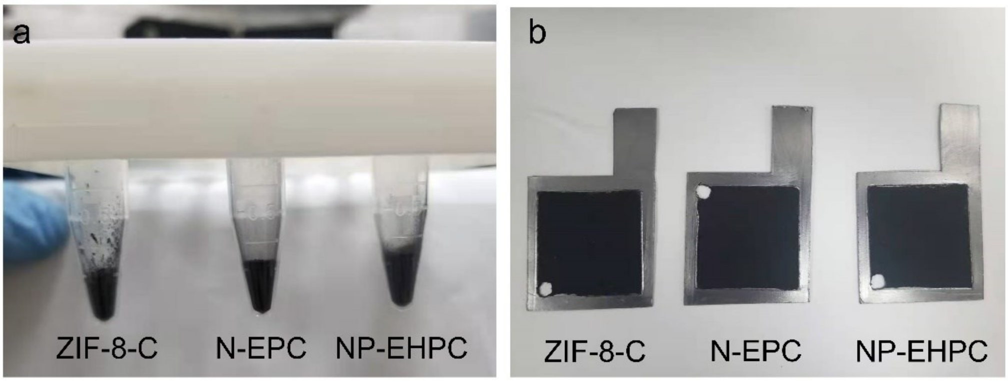

Fig. S9. Digital photographs of (a) ZIF-8, N-EPC, and NP-EHPC (50 mg each) and (b) the corresponding CDI electrodes fabricated from these materials (25 mg each).

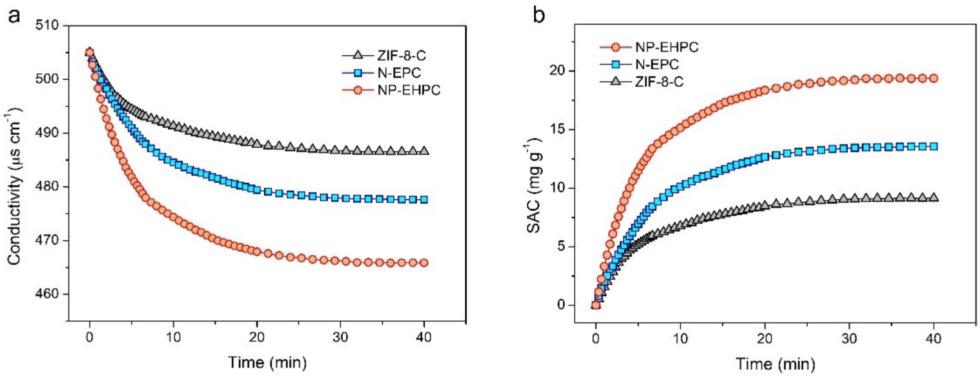

Fig. S10. (a) Conductivity profiles and (b) deionization capacities of ZIF-8-C, N-EPC, and NP-EHPC electrodes in 250 mg L^{-1} NaCl solutions at 1.2 V.

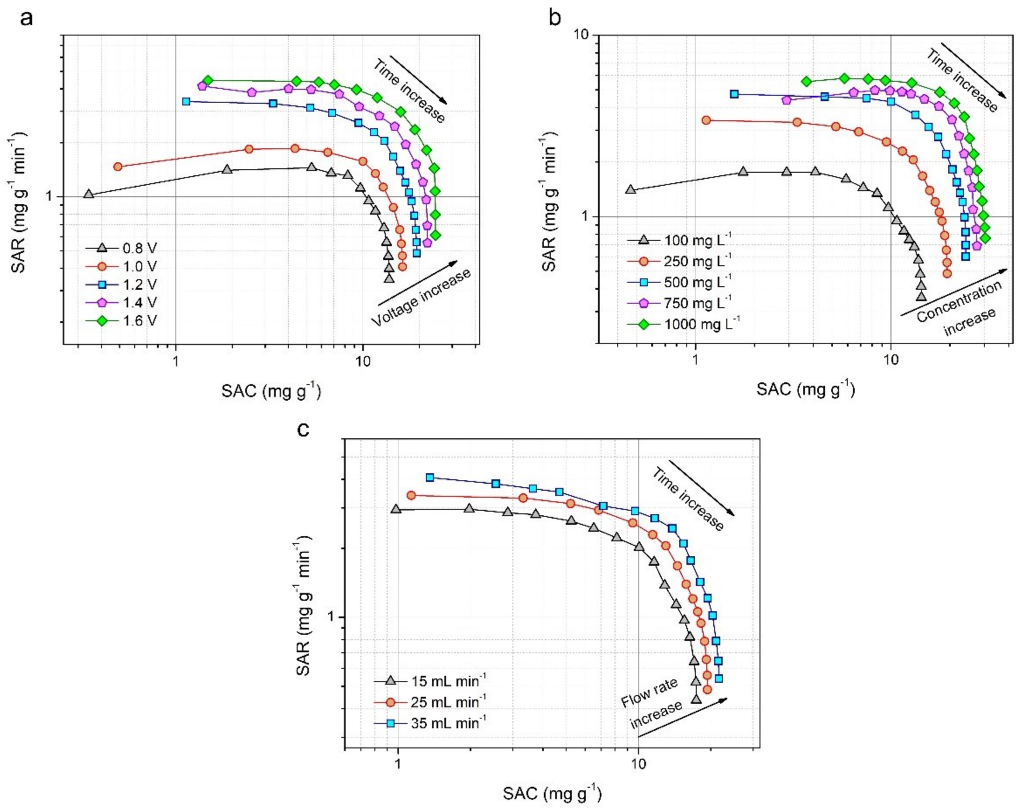

Fig. S11. CDI Ragone plots of the NP-EHPC electrode (a) at different applied voltage in 250 mg L^{-1} NaCl solution, (b) in different initial concentration of NaCl solution at 1.2 V, and (c) with different flow rate in 250 mg L^{-1} NaCl solution at 1.2 V.

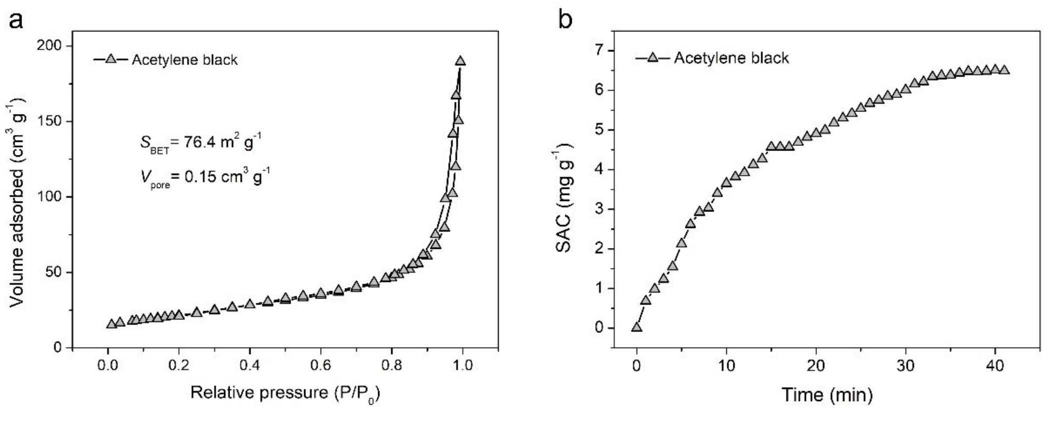

Fig. S12. (a) N_2 adsorption-desorption isotherms of acetylene black. (b) Deionization capacities of acetylene black in 500 mg L^{-1} NaCl solutions at 1.2 V.

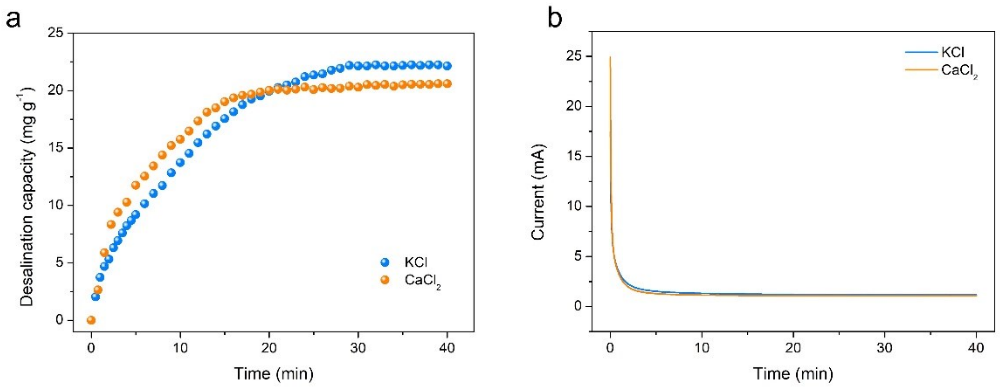

Fig. S13. (a) Desalination capacity *vs.* time curves of the NP-EHPC electrode in KCl and $CaCl_2$ solutions at 1.2 V. (b) Current response curves of the NP-EHPC electrode in 4.28 mM KCl and $CaCl_2$ solutions at 1.2 V.

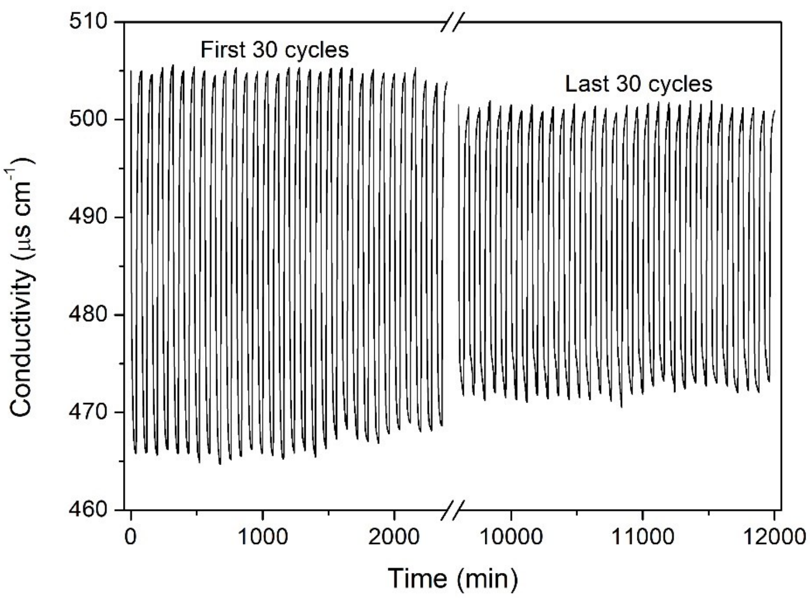

Fig. S14. Regeneration test of the NP-EHPC electrode over 150 cycles in a 250 mg L^{-1} NaCl solution at a charge/discharge voltage of 1.2/0 V.

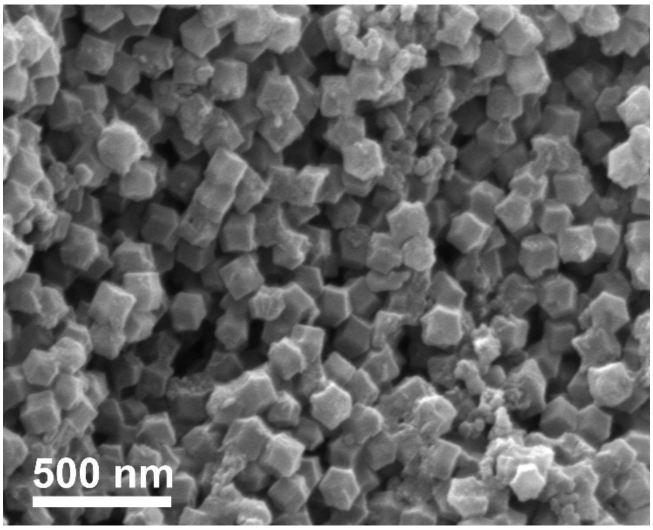

Fig. S15. SEM of NP-EHPC after the 150 regeneration cycles.

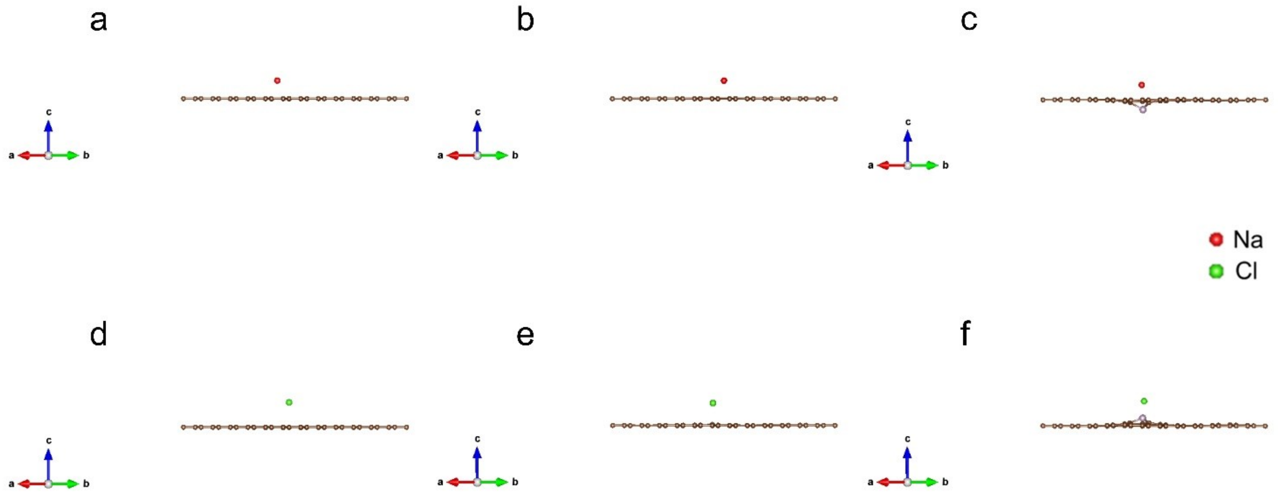

Fig. S16. Side views of Na and Cl atoms adsorbed on (a, d) monolayer graphene, (b, e) N-doped graphene, and (c, f) N, P co-doped graphene.

Note: Theoretical calculations

All the calculations were performed using density functional theory (DFT) with the projector augmented plane-wave method, as implemented in the Vienna *ab initio* simulation package.[15] The generalized gradient approximation proposed by Perdew, Burke, and Ernzerhof was selected for the exchange-correlation potential.[16] The long-range van der Waals interaction is described by the DFT-D3 approach.[17] The cut-off energy for plane wave was set to 400 eV. The energy criterion was set to 10^{-5} eV in the iterative solution of the Kohn-Sham equation. The Brillouin zone integration was performed by 2×2×1 k-mesh. All the structures were relaxed until the residual forces on the atoms have declined to less than 0.05 eV/Å. Supercells containing 6×6×1 unit cell were built to investigate the adsorption of Na and Cl on undoped, N-doped, and N, P co-doped graphene. A vacuum layer of 15 Å was added vertical to the sheet. The adsorption energy is defined as follows,

$$E_a = E_{graphene + Na/Cl} - E_{graphene} - E_{Na/Cl}$$

where $E_{\mathrm{graphene+Na/Cl}}$, E_{graphene}, and $E_{\mathrm{Na/Cl}}$ are total energies of undoped/doped graphene with adatom, undoped/doped graphene, and adatom in the bulk or gas, respectively.

References

1 G. Zhu, H. Wang, H. Xu and L. Zhang, *J. Electroanal. Chem.*, 2018, **822**, 81-88.

2 N. Pugazhenthiran, S. S. Gupta, A. Prabhath, M. Manikandan, J. R. Swathy, V. K. Raman and T. Pradeep, *ACS Appl. Mater. Interfaces*, 2015, **7**, 20156-20163.

3 J. Zhang, J. Fang, J. Han, T. Yan, L. Shi and D. Zhang, *J. Mater. Chem. A*, 2018, **6**, 15245-15252.

4 H. Yin, S. Zhao, J. Wan, H. Tang, L. Chang, L. He, H. Zhao, Y. Gao and Z. Tang, *Adv. Mater.*, 2013, **25**, 6270-6276.

5 Z. Wang, X. Xu, J. Kim, V. Malgras, R. Mo, C. Li, Y. Lin, H. Tan, J. Tang, L. Pan, Y. Bando, T. Yang and Y. Yamauchi, *Mater. Horiz.*, 2019, **6**, 1433-1437.

6 Y. Zhao, G. Luo, L. Zhang, L. Gao, D. Zhang and Z. Fan, *Electrochim. Acta*, 2020, **331**, 135420.

7 M. Wang, X. Xu, J. Tang, S. Hou, M. S. A. Hossain, L. Pan and Y. Yamauchi, *Chem. Commun.*, 2017, **53**, 10784-10787.

8 W. Dianbudiyanto and S. H. Liu, *Desalination*, 2019, **468**, 114069.

9 T. Liu, J. Serrano, J. Elliott, X. Yang, W. Cathcart, Z. Wang, Z. He and G. Liu, *Sci. Adv.*, 2020, **6**, eaaz0906.

10 Y. Zhu, G. Zhang, C. Xu and L. Wang, *ACS Appl. Mater. Interfaces*, 2020, **12**, 29706-29716.

11 C. C. Hsu, Y. H. Tu, Y. H. Yang, J. A. Wang and C. C. Hu, *Desalination*, 2020, **481**, 114362.

12 X. Xu, J. Tang, Y. V. Kaneti, H. Tan, T. Chen, L. Pan, T. Yang, Y. Bando and Y. Yamauchi, *Mater. Horiz.*, 2020, **7**, 1404-1412.

13 L. Liu, C. Zhao, F. Zheng, D. Deng, M. A. Anderson and Y. Wang, *Desalination*, 2021, **498**, 114794.

14 J. J. Lado, R. L. Zornitta, I. V. Rodríguez, K. M. Barcelos and L. A. M. Ruotolo, ACS *Sustainable Chem. Eng.*, 2019, **7**, 18992-19004.

15 G. Kresse and D. Joubert, *Phys. Rev. B*, 1999, **59**, 1758-1775.

16 J. P. Perdew, K. Burke and M. Ernzerhof, *Phys. Rev. Lett.*, 1996, **77**, 3865-3868.

17 S. Grimme, J. Antony, S. Ehrlich and H. Krieg, *J. Chem. Phys.*, 2010, **132**, 154104.